

Population pharmacokinetics and pharmacogenetics of ritonavir-boosted darunavir in the presence of raltegravir or tenofovir disoproxil fumarate/emtricitabine in HIV-infected adults and the relationship with virological response: a sub-study of the NEAT001/ANRS143 randomized trial

Laura Dickinson^{1*}, Rohan Gurjar¹, Wolfgang Stöhr², Stefano Bonora³, Andrew Owen¹, Antonio D'Avolio³, Adam Cursley², Jean-Michel Molina⁴, Gerd Fäetkenheuer⁵, Linos Vandekerckhove⁶, Giovanni Di Perri³, Anton Pozniak⁷, Laura Richert⁸, François Raffi⁹ and Marta Boffito^{7,10} on behalf of the NEAT001/ANRS143 Study Group†

¹Department of Molecular & Clinical Pharmacology, University of Liverpool, Liverpool, UK; ²Medical Research Council Clinical Trials Unit at University College London, London, UK; ³University of Turin, Unit of Infectious Diseases, Turin, Italy; ⁴University of Paris, Diderot Infectious Diseases, Paris, France; ⁵University Köln, Unit of Internal Medicine, Köln, Germany; ⁶Ghent University and Ghent University Hospital, HIV Translational Research Unit, Ghent, Belgium; ⁷Chelsea and Westminster NHS Trust, London, UK; ⁸University of Bordeaux, INSERM, Bordeaux Population Health Research Center, UMR 1219, Bordeaux, France; ⁹Nantes University Hospital, Infectious and Tropical Diseases, Nantes, France; ¹⁰Imperial College London, London, UK

*Corresponding author. E-mail: laurad@liverpool.ac.uk
†Members are listed in the Acknowledgements.

Received 11 July 2019; returned 6 September 2019; revised 11 October 2019; accepted 21 October 2019

Objectives: NEAT001/ANRS143 demonstrated non-inferiority of once-daily darunavir/ritonavir (800/100 mg) + twice-daily raltegravir (400 mg) versus darunavir/ritonavir + tenofovir disoproxil fumarate/emtricitabine (245/200 mg once daily) in treatment-naïve patients. We investigated the population pharmacokinetics of darunavir, ritonavir, tenofovir and emtricitabine and relationships with demographics, genetic polymorphisms and virological failure.

Methods: Non-linear mixed-effects models (NONMEM v. 7.3) were applied to determine pharmacokinetic parameters and assess demographic covariates and relationships with SNPs (*SLCO3A1*, *SLCO1B1*, *NR1I2*, *NR1I3*, *CYP3A5*3*, *CYP3A4*22*, *ABCC2*, *ABCC10*, *ABCG2* and *SCL47A1*). The relationship between model-predicted darunavir AUC_{0–24} and C₂₄ with time to virological failure was evaluated by Cox regression.

Results: Of 805 enrolled, 716, 720, 347 and 361 were included in the darunavir, ritonavir, tenofovir and emtricitabine models, respectively (11% female, 83% Caucasian). No significant effect of patient demographics or SNPs was observed for darunavir or tenofovir apparent oral clearance (CL/F); coadministration of raltegravir did not influence darunavir or ritonavir CL/F. Ritonavir CL/F decreased by 23% in *NR1I2* 63396C>T carriers and emtricitabine CL/F was linearly associated with creatinine clearance ($P<0.001$). No significant relationship was demonstrated between darunavir AUC_{0–24} or C₂₄ and time to virological failure [HR (95% CI): 2.28 (0.53–9.80), $P=0.269$; and 1.82 (0.61–5.41), $P=0.279$, respectively].

Conclusions: Darunavir concentrations were unaltered in the presence of raltegravir and not associated with virological failure. Polymorphisms investigated had little impact on study-drug pharmacokinetics. Darunavir/ritonavir + raltegravir may be an appropriate option for patients experiencing NRTI-associated toxicity.

Introduction

HIV therapy commonly consists of two NRTIs combined with an integrase inhibitor, NNRTI or boosted PI.¹ However, renal and

bone-associated adverse events, particularly with tenofovir,^{2,3} and concerns regarding cardiovascular risk with abacavir, have led to exploration of NRTI-sparing regimens as alternatives for

treatment-naïve patients. NEAT001/ANRS143, a Phase III, randomized, open-label trial, demonstrated non-inferiority of raltegravir (400 mg twice daily) + darunavir/ritonavir (800/100 mg once daily) compared with tenofovir disoproxil fumarate/emtricitabine (245/200 mg once daily) + darunavir/ritonavir (800/100 mg once daily) in a large group of European treatment-naïve patients [Kaplan–Meier-estimated treatment failure from the primary ITT analysis at 96 weeks was 17.8% (NRTI-sparing) versus 13.8% (standard regimen)]. The adjusted difference in treatment failure between study arms was 4.0% (95% CI -0.8 to 8.8) and the HR for attaining the primary endpoint with the NRTI-sparing regimen was 1.34 (95% CI 0.96 – 1.88). The NRTI-sparing regimen was well tolerated but was not recommended in patients with CD4 counts <200 cells/mm³ due to increased risk of virological failure.⁴

This analysis investigated the interplay between patient characteristics, SNPs, pharmacokinetics and pharmacodynamics (efficacy and renal adverse events) in the large NEAT001/ANRS143 trial, with a focus on darunavir, ritonavir, tenofovir and emtricitabine.

Methods

Patients and pharmacokinetic sampling

NEAT001/ANRS143 has previously been described.⁴ In summary, HIV-infected, treatment-naïve patients were recruited between August 2010 and September 2011 from 15 European countries (78 sites). Individuals were eligible if their plasma HIV-1 viral load was >1000 copies/mL, CD4 count was <500 cells/mm³ (except patients with symptomatic HIV infection) and there was no previous or current evidence of major IAS-USA resistance mutations. Patients suffering from or requiring treatment for active opportunistic infections (e.g. tuberculosis, hepatitis B/C), pregnant women and those with abnormal laboratory parameters or hepatic/renal impairment were excluded.

Patients were randomized (1:1) to receive ritonavir-boosted darunavir with either tenofovir disoproxil fumarate/emtricitabine (standard regimen) or raltegravir (NRTI-sparing regimen).⁴ Timed, single blood samples were drawn at Weeks 4 and 24 and plasma drug concentrations quantified by fully validated HPLC-MS and LC-MS methods^{5,6} with lower limits of quantification (LLQ) of 0.0391, 0.0098, 0.0156 and 0.0117 mg/L for darunavir, ritonavir, tenofovir and emtricitabine, respectively.

Ethics

Ethical approval was obtained from all study sites and the study conducted in accordance with the Declaration of Helsinki. All participants provided written informed consent.⁴

Genotyping

Total genomic DNA was extracted from patient blood using the QIAamp DNA Mini Kit (QIAGEN, West Sussex, UK) according to the manufacturer's instructions. The following SNPs, associated with metabolism and transport, were genotyped for darunavir and ritonavir: *SLCO3A1* G>A (rs4294800), *SLCO3A1* G>T (rs8027174), *SLCO1B1* 521T>C (rs4149056), *NR1I2* (PXR) 63396C>T (rs2472677), *NR1I3* (CAR) 540G>A (rs2307424), *CYP3A5**3 6986A>G (rs776746) and *CYP3A4**22 522–191C>T (rs35599367); for tenofovir: *ABCC2* (MRP2) 24C>T (rs717620), *ABCC2* 1249G>A (rs2273697), *ABCC10* (MRP7) 526G>A (rs9349256), *ABCC10* 2843T>C (rs2125739) and *ABCG2* 421C>A (rs2231142); and for emtricitabine: *SCL47A1* (MATE1) 922–158G>A (rs2289669) using real-time PCR allelic discrimination assays (Applied Biosystems, Foster City, CA, USA; Table S1, available as [Supplementary data](#) at JAC Online), essentially as described previously.⁷

Population pharmacokinetic modelling

Non-linear mixed-effects modelling (NONMEM v. 7.3, ICON Development Solutions, Ellicott City, MD, USA) implementing FOCE-I was applied to concentration–time data of each drug.⁸ With one sample per patient on each sampling occasion (Weeks 4 and 24), parameter estimates from the literature were used as priors for darunavir, ritonavir and emtricitabine^{9,10} (SPRIOR subroutine of NONMEM); tenofovir did not require priors, but parameter estimates from the literature were used initially.¹¹

The impact of covariates including bodyweight, age, sex, ethnicity, treatment backbone (i.e. tenofovir disoproxil fumarate/emtricitabine versus raltegravir; for darunavir/ritonavir), creatinine clearance (CL_{CR} , estimated using the Cockcroft–Gault equation; for tenofovir and emtricitabine) and the polymorphisms described above were evaluated on apparent oral clearance (CL/F). Genotypes were parameterized in the models to compare heterozygotes and homozygotes for the rare alleles to homozygotes for the common alleles as reference populations. If the proportion of homozygotes for the rare allele was $<10\%$ they were combined with the heterozygotes. Likewise, heterozygotes and homozygotes for the rare alleles were combined into one category if changes in CL/F were similar when compared with homozygotes for the common allele. Initially, univariable associations were assessed, followed by multivariable if more than one covariate was found to be significant (see below for statistical criteria).

A decrease in the minimal objective function value (OFV; $-2 \log$ likelihood) of at least 3.84 units was required to accept a model with an extra parameter ($P=0.05$, χ^2 distribution, 1 *df*). Once significant covariates were incorporated, backwards elimination was performed and biologically plausible covariates generating an increase in OFV of at least 10.83 units ($P=0.001$, χ^2 distribution, 1 *df*) were retained. This threshold was chosen in order to robustly test the relationships observed, given the large sample size but sparseness of the pharmacokinetic data per individual.

Model evaluation was performed by means of prediction-corrected visual predictive checks (pcVPCs)¹² constructed from 1000 simulations of each dataset implemented through Perl-speaks-NONMEM (PsN; v. 3.4.2)¹³ and plots developed using Xpose^{4,14} in RStudio (v. 1.1.383). The use of pcVPC corrects for the inclusion of significant covariates and/or varying dosages per drug.

For each drug secondary pharmacokinetic parameters, AUC_{0-24} , C_{max} and C_{24} , were derived for each patient and applied to the analyses incorporating virological response (outlined below). Ritonavir parameters were calculated using standard one-compartment pharmacokinetic equations for multiple oral dosing (Table S2). For the two-compartment drugs (darunavir, tenofovir and emtricitabine) full pharmacokinetic profiles were simulated for each patient per drug using their individual predicted model parameters. C_{max} and C_{24} were determined directly from the profiles and AUC_{0-24} as outlined (Table S2).

Pharmacokinetic–pharmacodynamic analysis

The primary pharmacodynamic endpoint was protocol-defined virological failure that included change of any component of the randomized regimen before Week 32 because of insufficient virological response (reductions of $<1 \log_{10}$ copies/mL in HIV-1 RNA by Week 18 or HIV-1 RNA ≥ 400 copies/mL at Week 24); failure to achieve virological response by Week 32 (HIV-1 RNA ≥ 50 copies/mL); and HIV-1 RNA ≥ 50 copies/mL at any time after Week 32. All virological components of the primary endpoint had to be confirmed by a second measurement.⁴ The association between model-predicted \log_{10} (C_{24}) or \log_{10} (AUC_{0-24}) and time to virological failure by Week 96 was evaluated using multivariable Cox regression, adjusting for sex, age, mode of HIV infection, ethnicity, country, baseline CD4 count, baseline HIV-1 RNA and drug regimen. Similarly, we also investigated the association of pharmacokinetic parameters with the primary endpoint of the NEAT001/ANRS143 trial, which was time to virological or clinical failure.⁴

The primary analyses were as randomized and based on available data. We also performed sensitivity analyses: (i) censoring analysis time when

Table 1. Clinical characteristics and demographics of patients included in the population pharmacokinetic models for the NEAT001/ANRS143 pharmacokinetic sub-study stratified by study drug

Parameter	Darunavir	Ritonavir	Tenofovir	Emtricitabine
Included for modelling (<i>n</i>)	716	720	347	361
Sex, <i>n</i> (%)				
male	634 (88.5)	637 (88.5)	309 (89.0)	321 (88.9)
female	81 (11.3)	82 (11.4)	37 (10.7)	39 (10.8)
transgender	1 (0.1)	1 (0.1)	1 (0.3)	1 (0.3)
Age (years)	38 (18–76)	37 (18–76)	39 (18–76)	38 (18–76)
Weight (kg)	72 (41–135)	72 (41–135)	73 (44–125)	73 (44–125)
CL _{CR} (mL/min)	115 (48–222)	115 (48–222)	116 (48–198)	116 (48–198)
CD4+ T cell count (cells/mm ³)	334 (4–780)	334 (4–780)	328 (4–685)	331 (4–685)
HIV-RNA (log ₁₀ copies/mL)	4.79 (3.11–6.53)	4.79 (3.11–6.53)	4.79 (3.15–6.53)	4.77 (3.13–6.53)
Randomization arm, <i>n</i> (%)				
tenofovir disoproxil fumarate/emtricitabine	359 (50.1)	361 (50.1)	347 (100)	361 (100)
raltegravir	357 (49.9)	359 (49.9)	—	—
Mode of HIV infection, <i>n</i> (%)				
homosexual/bisexual	499 (69.7)	502 (69.7)	246 (70.9)	259 (71.7)
heterosexual	165 (23.0)	166 (23.1)	80 (23.1)	80 (22.2)
other	52 (7.3)	52 (7.2)	21 (6.1)	22 (6.1)
Ethnicity, <i>n</i> (%)				
Caucasian	596 (83.2)	600 (83.3)	290 (83.6)	302 (83.7)
Black	78 (10.9)	78 (10.8)	34 (9.8)	34 (9.4)
Asian	18 (2.5)	18 (2.5)	8 (2.3)	10 (2.8)
other	24 (3.4)	24 (3.3)	15 (4.3)	15 (4.2)

Data expressed as median (range) unless stated otherwise.

any component of the initial randomized treatment was stopped; and (ii) multiple imputation of missing pharmacokinetic parameters (using the same factors as described above plus the event indicator and the Nelson–Aalen estimator¹⁵).

Additionally, we examined the association of CD4 count change from baseline to Week 96 with C₂₄ or AUC_{0–24} using multivariable linear regression models adjusting for baseline CD4 cell count and other factors as above.

Renal adverse events

For tenofovir, we examined the association between model-predicted C_{max} or AUC_{0–24} and the tenofovir SNPs with reduced glomerular function defined as at least 25% reduction from baseline in CL_{CR} sustained in two measurements at least 4 weeks apart. Multivariable Cox models were used, adjusting for sex, age, ethnicity, baseline CD4 count, baseline HIV-1 RNA and baseline CL_{CR}.

Results

Patients and sampling

Of 805 patients enrolled, data were available from 770 patients (*n*=386 in raltegravir arm; *n*=384 in tenofovir disoproxil fumarate/emtricitabine arm) totalling 1460 samples (*n*=726 in raltegravir arm; *n*=734 in tenofovir disoproxil fumarate/emtricitabine arm). Between 10% and 25% of samples were excluded due to the lack of recorded time post-dose, missing concentration, time post-dose >30h, sample below assay LLQ or a combination thereof. Overall, 1317 and 1283 concentrations were used to develop darunavir and ritonavir models in a total of 716 and 720 patients,

respectively. The majority of patients received darunavir/ritonavir 800/100 mg once daily (*n*=698, 97%); alternative doses were recorded for a small proportion (*n*=18; Table S3). For tenofovir and emtricitabine, 347 (588 concentrations) and 361 patients (656 concentrations) were included, respectively. Patient demographics and clinical characteristics are summarized in Table 1. Patients excluded from pharmacokinetic modelling had similar characteristics to included patients apart from ethnicity and country.

Genotyping

Of the patients with complete pharmacokinetic data for darunavir, ritonavir, tenofovir and emtricitabine, 618/716, 621/720, 302/347 and 314/361 (86%–87%), respectively, had a blood sample for genotyping. Genotyping assays failed in one and three patients, respectively, for ABCC2 24C>T and ABCC10 526G>A; therefore, 301 and 299 patients had both pharmacokinetic and genetic data for these particular SNPs. All genotypes were in Hardy–Weinberg equilibrium with the exception of SLCO3A1 G>T (rs8027174) and CYP3A5*3 (rs776746) and could not be evaluated in the covariate model; allele frequencies are summarized (Table 2).

Darunavir/ritonavir population pharmacokinetic modelling

Darunavir and ritonavir plasma concentrations are presented (Figure 1a and b) and were 0.06–16.4 and 0.01–2.76 mg/L, respectively, over 0.17–30.1 h post-dose. Due to extensive model run times, darunavir and ritonavir were ultimately modelled

Table 2. Allele frequencies for the SNPs investigated for the NEAT001/ANRS143 pharmacokinetic sub-study associated with metabolism and transport of the study drugs

SNP	Darunavir	Ritonavir	Tenofovir	Emtricitabine
Number of patients (n)	716	720	347	361
<i>SLCO3A1</i> G>A (rs4294800)				
GG	302 (42.2)	303 (42.1)		
GA	255 (35.6)	257 (35.7)		
AA	61 (8.5)	61 (8.5)		
missing	98 (13.7)	99 (13.8)		
<i>SLCO3A1</i> G>T (rs8027174)				
GG	520 (72.6)	522 (72.5)		
GT	98 (13.7)	99 (13.8)		
TT	0 (0.0)	0 (0.0)		
missing	98 (13.7)	99 (13.8)		
<i>SLCO1B1</i> 521T>C (rs4149056)				
TT	445 (62.2)	446 (61.9)		
CT	162 (22.6)	164 (22.8)		
CC	11 (1.5)	11 (1.5)		
missing	98 (13.7)	99 (13.8)		
<i>NR1I2</i> 63396C>T (rs2472677)				
CC	125 (17.5)	125 (17.4)		
CT	296 (41.3)	299 (41.5)		
TT	197 (27.5)	197 (27.4)		
missing	98 (13.7)	99 (13.8)		
<i>NR1I3</i> 540G>A (rs2307424)				
GG	294 (41.1)	296 (41.1)		
GA	258 (36.0)	258 (35.8)		
AA	66 (9.2)	67 (9.3)		
missing	98 (13.7)	99 (13.8)		
<i>CYP3A5</i> *3 6986A>G (rs776746)				
CC	448 (62.6)	450 (62.5)		
CT	127(17.7)	127 (17.6)		
TT	43(6.0)	44 (6.1)		
missing	98 (13.7)	99 (13.8)		
<i>CYP3A4</i> *22 522-191C>T (rs35599367)				
GG	574 (80.2)	577 (80.1)		
GA	44 (6.1)	44 (6.1)		
AA	0 (0.0)	0 (0.0)		
missing	98 (13.7)	99 (13.8)		
<i>ABCC2</i> 24C>T (rs717620)				
CC			210 (60.5)	
CT			80 (23.1)	
TT			11 (3.2)	
missing			46 (13.3)	
<i>ABCC2</i> 1249G>A (rs2273697)				
GG			188 (54.2)	
GA			100 (28.8)	
AA			14 (4.0)	
missing			45 (13.0)	
<i>ABCC10</i> 526G>A (rs9349256)				
GG			110 (31.7)	
GA			138 (39.8)	
AA			51 (14.7)	
missing			48 (13.8)	

Continued

Table 2. Continued

SNP	Darunavir	Ritonavir	Tenofovir	Emtricitabine
ABCC10 2843T>C (rs2125739)				
TT			170 (49.0)	
CT			113 (32.6)	
CC			19 (5.5)	
missing			45 (13.0)	
ABCG2 421C>A (rs2231142)				
CC			251 (72.3)	
CA			47 (13.5)	
AA			1 (0.3)	
missing			48 (13.8)	
SCL47A1 922-158G>A (rs2289669)				
GG				108 (29.9)
GA				163 (45.2)
AA				43 (11.9)
missing				47 (13.0)

Values are expressed as *n* (%).

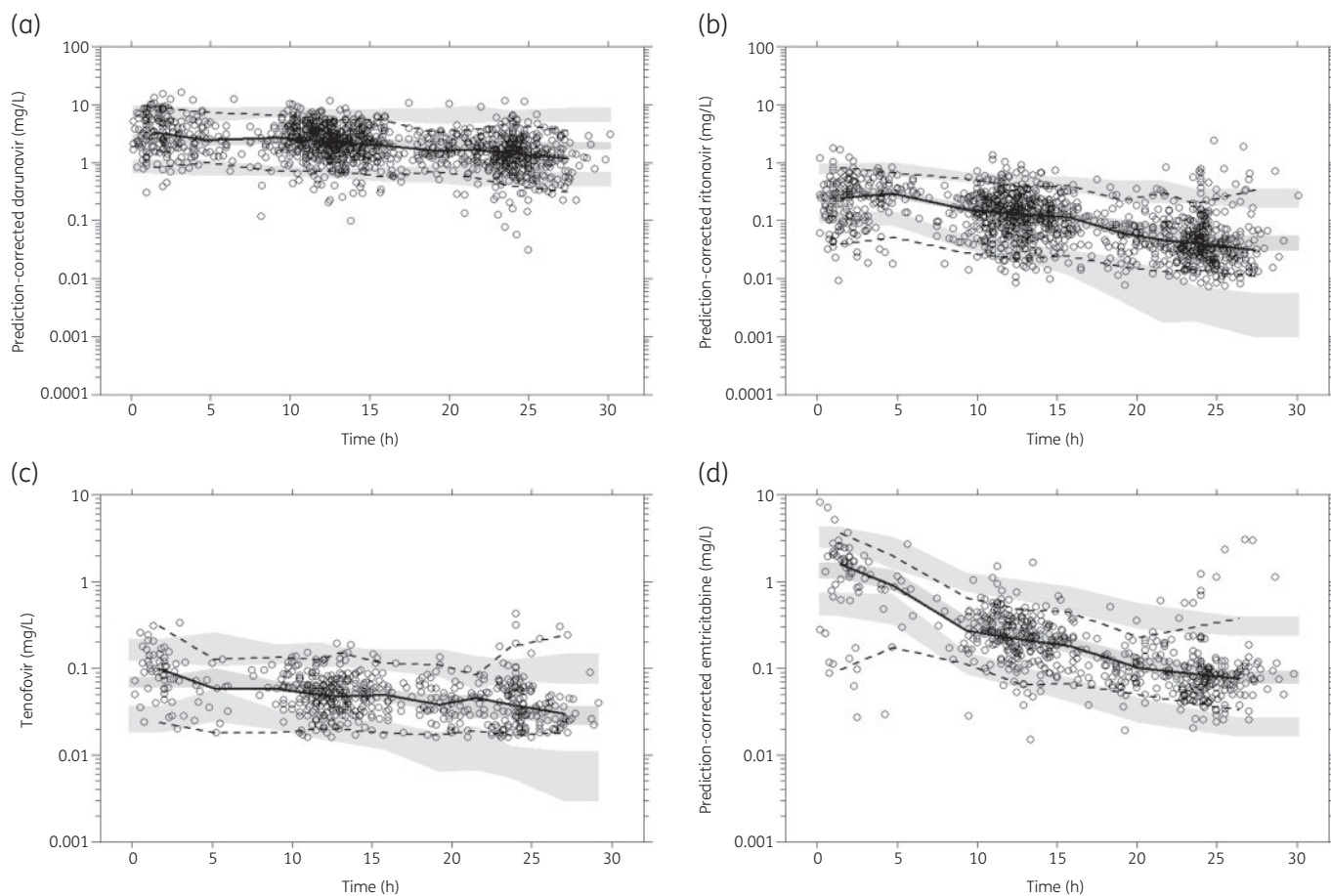


Figure 1. VPC for (a) darunavir, (b) ritonavir, (c) tenofovir and (d) emtricitabine. Plots for darunavir, ritonavir and emtricitabine are pcVPC. The lines represent the percentiles of the observed data (P5, P50, P95) and the shaded areas the 95% CI of the simulated data. Observed concentration–time data for darunavir (*n*=716 patients, 1317 concentrations), ritonavir (*n*=720 patients, 1283 concentrations), tenofovir (*n*=347 patients, 588 concentrations) and emtricitabine (*n*=361 patients, 656 concentrations) are superimposed (open circles).

Table 3. Population pharmacokinetic parameter estimates and relative standard errors (RSEs) derived from the final models for darunavir, ritonavir, tenofovir and emtricitabine

Parameter	Parameter estimate (RSE%)			
	darunavir	ritonavir	tenofovir	emtricitabine
Number of patients (n)	716	720	347	361
Fixed effects				
CL/F (L/h)	14.6 (2.3)	20.7 (2.4)	101 (3.3)	17.0 (2.7)
V/F or V_c/F (L)	41.4 (5.7)	278 (13.7)	402 (67.7)	36.8 (3.2)
Q/F (L/h)	30.4 (2.4)	—	700 (21.1)	5.6 (14.3)
V_p/F (L)	1130 (0.2)	—	2910 (18.7)	58.8 (2.3)
k_a (h^{-1})	0.30 (5.4)	0.95 (17.5)	1.18 (64.2)	0.35 (15.4)
Ritonavir–darunavir interaction				
IC ₅₀ (mg/L)	0.42 (10.2)	—	—	—
I_{max}	1.00 fixed	—	—	—
Random effects				
IIV CL/F (%)	37.4 (8.5)	47.7 (17.2)	37.8 (16.6)	27.5 (28.1)
IIV V_c/F (%)	—	—	—	84.1 (32.5)
Residual error				
proportional (%)	48.5 (4.4)	49.9 (5.3)	37.1 (7.8)	41.8 (8.4)
Covariates				
θ_{weight} CL/F	—	0.75 fixed	—	—
θ_{weight} V/F	—	1.00 fixed	—	—
$\theta_{CT/TT}$ CL/F	—	1.23 (5.6)	—	—
θ_{MISS} CL/F	—	1.24 (7.5)	—	—
θ_{CLCR} CL/F	—	—	—	0.0037 (21.9)

RSE is calculated as $(SE_{ESTIMATE}/ESTIMATE) \times 100$.

IC₅₀, ritonavir concentration associated with 50% maximum inhibition of darunavir CL/F; I_{max} , maximum inhibitory effect of ritonavir; θ_{weight} , allometric scaling factors associated with changes in ritonavir CL/F and V/F with bodyweight; $\theta_{CT/TT}$, θ_{MISS} , relative changes in ritonavir CL/F for *NR112* 63396CT/TT (heterozygote and homozygote mutant) and missing *NR112* 63396C>T genotype compared to the reference, *NR112* 63396CC (WT); θ_{CLCR} , factor associated with the linear relationship between emtricitabine CL/F and CL_{CR}.

sequentially.¹⁶ Firstly, ritonavir was modelled, followed by darunavir with ritonavir concentrations calculated within the darunavir model using the individual posterior parameter estimates from the final ritonavir model (see below).

A one-compartment model with first-order absorption best described ritonavir, parameterized by CL/F, apparent volume of distribution (V/F) and absorption rate constant (k_a); a literature prior was included for CL/F.⁹ Interindividual variability (IIV) was estimated on CL/F but interoccasion variability (IOV) was not supported; a proportional model best described residual error. Darunavir was described by a two-compartment model parameterized by CL/F, volume of distribution of the central and peripheral compartments (V_c/F , V_p/F), intercompartmental clearance (Q/F) and k_a . The interaction between ritonavir and darunavir was via a direct-response model with ritonavir concentrations inhibiting darunavir CL/F parameterized by IC₅₀ (ritonavir concentration associated with 50% maximum inhibition) and I_{max} (maximum inhibitory effect, fixed to 1). IIV was included on darunavir CL/F and a proportional residual error was used.

Univariable analysis identified antiretroviral backbone as a significant covariate on darunavir CL/F. Compared with tenofovir disoproxil fumarate/emtricitabine, raltegravir increased darunavir CL/F by 11% (Δ OFV -10.47). Furthermore, *NR112* 63396C>T was significantly associated with darunavir CL/F (Δ OFV -6.82).

Following multivariable analysis, none of the covariates remained in the model. Weight (allometrically scaled and centred on 70 kg), *NR112* 63396C>T, *NR113* 540G>A, *CYP3A5*3* and *SLCO3A1* rs8027174 G>T were significantly associated with ritonavir CL/F, with weight and *NR112* 63396C>T retained in the model at the $P < 0.001$ significance level (χ^2 distribution) following forwards inclusion, backwards elimination. Ritonavir CL/F was increased by 23% in *NR112* 63396T allele carriers compared with C allele homozygotes. Model parameters and pcVPCs for darunavir and ritonavir are presented (Table 3 and Figure 1a and b). Goodness-of-fit plots are also shown (Figures S1 and S2).

Tenofovir and emtricitabine population pharmacokinetic modelling

Tenofovir and emtricitabine plasma concentrations are shown (Figure 1c and d) and were 0.016–0.42 mg/L for tenofovir and 0.013–4.67 mg/L for emtricitabine (0.17–29.8 h post-dose).

Tenofovir and emtricitabine were described by two-compartment models with first-order absorption. Tenofovir concentrations were lower than those previously reported in the literature and therefore priors were unlikely to be informative; adjustment of starting estimates appeared sufficient. Literature priors were used for emtricitabine fixed effects with the exception

Table 4. Mean (\pm SD) individual model-predicted secondary pharmacokinetic parameters for darunavir, ritonavir (800/100 mg once daily), tenofovir (245 mg once daily; dosed as disoproxil fumarate) and emtricitabine (200 mg once daily)

Parameter	Darunavir		Ritonavir		Tenofovir	Emtricitabine
	arm 1	arm 2	arm 1	arm 2		
Number of patients (n)	345	353	345	353	347	361
AUC ₀₋₂₄ (mg·h/L)	57.42 (17.84)	55.48 (19.74)	4.24 (1.97)	4.32 (3.35)	1.43 (0.60)	11.84 (3.54)
CV (%)	31	36	46	78	42	30
C _{max} (mg/L)	5.35 (0.88)	5.25 (0.97)	0.28 (0.10)	0.28 (0.15)	0.13 (0.03)	1.50 (0.19)
CV (%)	16	18	35	55	19	12
C ₂₄ (mg/L)	1.75 (0.73)	1.68 (0.80)	0.07 (0.07)	0.07 (0.12)	0.04 (0.02)	0.10 (0.13)
CV (%)	41	48	98	166	59	135

Darunavir and ritonavir parameters are stratified by randomization arm, i.e. antiretroviral backbone (arm 1: tenofovir disoproxil fumarate/emtricitabine; arm 2: raltegravir, NRTI-sparing).

CV, coefficient of variation; C₂₄, concentration 24 h post-dose (trough).

of k_{cat}.¹⁰ IIV was included for tenofovir CL/F and emtricitabine CL/F and V_c/F; a proportional error was applied for both models.

Black patients had 31% higher tenofovir CL/F compared with Caucasian, Asian and other ethnicity patients combined (Δ OFV –11.39; CL/F values similar for Asian/other versus Caucasian) and CL_{CR} was also significantly associated with tenofovir CL/F (Δ OFV –6.47). Tenofovir CL/F was decreased by 18% in ABCG2 421A allele carriers compared with C homozygotes (Δ OFV –11.26); none of the other SNPs showed significant relationships with tenofovir CL/F. Following multivariable analysis, ethnicity, CL_{CR} and ABCG2 421C>A did not remain in the model. Significant univariable associations were observed between several covariates and emtricitabine CL/F: CL_{CR} (linear), ethnicity [Asian versus Black, Caucasian, other (reference)], weight, age (linear) and SCL47A1 rs2289669 G>A [GG/GA (reference) versus AA]. Only CL_{CR} was retained in the emtricitabine model. Tenofovir and emtricitabine final model parameters are summarized (Table 3) and pcVPCs are shown (Figure 1c and d). Goodness-of-fit plots are also displayed (Figure S3 and S4, respectively).

Secondary pharmacokinetic parameters

Predicted AUC₀₋₂₄, C_{max} and C₂₄ for darunavir/ritonavir (stratified by antiretroviral backbone), tenofovir and emtricitabine are summarized (Table 4); darunavir/ritonavir doses other than 800/100 mg once daily are displayed separately (n=18; Table S3).

All patients had a predicted darunavir C₂₄ well above the protein binding-adjusted EC₅₀ for WT HIV-1 of 0.055 mg/L¹⁷ with C₂₄ values of 0.38–5.79 mg/L. Mean (\pm SD) predicted darunavir pharmacokinetic parameters were generally in agreement with those reported from the Phase III ARTEMIS trial¹⁷ and predicted emtricitabine AUC₀₋₂₄, C_{max} and C₂₄ were also consistent with previously reported values¹⁸ (Table S4). Mean tenofovir pharmacokinetic parameters were approximately 40%–60% lower than those reported for HIV patients when administered with a meal following multiple dosing (Table S4).¹⁹

Pharmacokinetic–pharmacodynamic analysis

The analysis of darunavir pharmacokinetic parameters and virological failure included 716 patients with 94 virological failures

(13.1%). We found no significant association of darunavir C₂₄ or AUC₀₋₂₄ with time to virological failure overall [multivariable HR: 1.82 per log₁₀ mg/L (95% CI 0.61–5.41), P=0.279; and 2.28 per log₁₀ mg·h/L (95% CI 0.53–9.80), P=0.269, respectively] nor evidence that this was different in the two arms (interaction P values: arm*C₂₄ P=0.679; arm*AUC₀₋₂₄ P=0.380). Results were similar when censoring after switch from allocated regimen, after multiple imputation of missing pharmacokinetic parameters or when analysing time to trial primary endpoint (results not shown).

Adding the corresponding pharmacokinetic parameters for tenofovir and emtricitabine to the model with participants of the darunavir/tenofovir disoproxil fumarate/emtricitabine arm did not reveal any significant associations [for example, HR per additional log₁₀ mg/L emtricitabine C₂₄ or tenofovir C₂₄: 1.63 (95% CI 0.50–5.37), P=0.421; and 1.46 (95% CI 0.27–8.00), P=0.661, respectively].

There was no association between darunavir pharmacokinetic parameters and change in CD4 cell count from randomization to Week 96 for either C₂₄ [26.6 (95% CI –66.8 to 119.9) cells/mm³ per log₁₀ mg/L increase, P=0.522] or AUC₀₋₂₄ [53.2 (95% CI –66.7 to 173.0) cells/mm³ per log₁₀ mg·h/L increase, P=0.329]. CD4 cell count post-randomization was also not associated with pharmacokinetic parameters of emtricitabine or tenofovir (results not shown).

Renal adverse events

Of 347 participants with tenofovir pharmacokinetic estimates, 10 (2.9%) experienced a decrease in glomerular function. Both higher AUC₀₋₂₄ and C_{max} were significantly associated with a higher risk, with an HR of 1.92 per additional mg·h/L (95% CI 1.20–3.05), P=0.006 and an HR of 4.65 per additional 0.1 mg/L (95% CI 1.54–14.08), P=0.007, respectively. No relationships were observed with polymorphisms in ABCG2, ABCC10 or ABCG2.

Discussion

Based on the pharmacokinetic analysis of NEAT001/ANRS143, no significant difference in once-daily darunavir/ritonavir CL/F was observed when coadministered with twice-daily raltegravir as an

NRTI-sparing regimen compared with the standard regimen containing tenofovir disoproxil fumarate/emtricitabine. Furthermore, no associations of virological failure or CD4 cell count with darunavir concentrations were detected.

Due to non-overlapping metabolic pathways between darunavir and raltegravir (CYP3A4 versus UGT1A1) the potential for predictable drug–drug interactions of clinical consequence is low. However, previous studies have demonstrated a moderate influence of raltegravir on darunavir pharmacokinetics, with one observing significantly lower C_{max} and AUC_{0-24} ($n=17$ with raltegravir, $n=8$ without raltegravir) but no change in C_{trough} ($n=31$ with raltegravir, $n=22$ without raltegravir),²⁰ and another reporting 40% lower darunavir concentrations in patients receiving darunavir + raltegravir compared with those without ($n=55$), but no impact on virological efficacy.²¹ In contrast, a small Phase I study did not observe any change in boosted darunavir when raltegravir was added to a regimen containing tenofovir disoproxil fumarate/emtricitabine; however, following removal of the NRTI backbone, darunavir C_{trough} decreased by 36%.²² NEAT001/ANRS143 was performed in a larger patient population and although darunavir CL/F was 11% higher in the presence of raltegravir, it did not reach statistical significance in the final model; moreover, model-predicted C_{24} values in all patients were well above the protein binding-adjusted EC_{50} for WT HIV-1 (0.055 mg/L).

In addition to demographic descriptors, we investigated the effect of polymorphisms governing expression and/or function of specific metabolic pathways and transporters. The *SLCO3A1* gene encodes expression of the influx transporter OATP3A1. Although darunavir is not a confirmed substrate, Moltó *et al.*⁹ observed 12% lower CL/F in carriers of the *SLCO3A1* rs4294800 A allele and a 2.5-fold higher V_d/F in *SLCO3A1* rs8027174 T allele homozygotes, although probably of more mechanistic than clinical relevance. We were unable to confirm these findings given that *SLCO3A1* rs4294800 G>A was not in Hardy–Weinberg equilibrium. Prevalence of *SLCO1B1* 521T>C is high in Caucasians and carriers of the C allele exhibit higher plasma lopinavir concentrations.²³ However, a relationship with darunavir in the present study was not established. *CYP3A4**22 (522–191C>T) and *CYP3A5**3 (6986A>G) are linked to low CYP3A4 expression and activity and loss of CYP3A5 function.^{24–26} HIV-infected patients homozygous for *CYP3A4**22 have previously been associated with a 53% reduction in ritonavir-boosted lopinavir CL/F and increased C_{trough} compared with homozygotes for the common allele,²⁷ whereas a small study in healthy volunteers determined significantly higher maraviroc CL/F and lower $AUC_{0-\infty}$ in those with fully functional CYP3A5 (*CYP3A5**1/*1; $n=8$) compared with dysfunctional homozygotes (*CYP3A5**3/*3 or *3/*6 or *6/*7; $n=8$).²⁸ Similar associations with darunavir pharmacokinetics and *CYP3A4**22 were not replicated in NEAT001/ANRS143 and *CYP3A5**3 could not be evaluated due to lack of Hardy–Weinberg equilibrium. Moreover, no significant relationships with patient characteristics were evident; however, derived pharmacokinetic parameters were generally consistent with those reported for a small group of treatment-naïve patients from the ARTEMIS trial.¹⁷

Ritonavir CL/F was not influenced by the evaluated SNPs with the exception of *NR1I2* 63396C>T. Carriers of the rare allele (CT/TT) exhibited an increased ritonavir CL/F of 23%, which is in agreement with the impact reported for unboosted atazanavir concentrations.²⁹ Bodyweight was significantly associated

with ritonavir CL/F, which is consistent with previous population pharmacokinetic analyses.^{9,30}

Model-predicted emtricitabine pharmacokinetic parameters were in agreement with literature values; however, observed tenofovir concentrations and hence predicted tenofovir secondary pharmacokinetic parameters were lower than previous studies. Differences could be the result of additional covariates not captured as part of the study, for example a food effect based on meal composition (consumption of a high-fat meal has been associated with enhanced tenofovir AUC and C_{max} compared with the fasted state).¹⁹ The bioanalytical laboratory participates in an external quality assurance programme³¹ with excellent performance, therefore assay or analytical equipment errors are unlikely to be a contributing factor.

Both tenofovir and emtricitabine are excreted relatively unchanged by the kidneys. Tenofovir is transported in the proximal tubule by ABCC4 (MRP4),³² ABCC10 (MRP7),³³ ABCC11 (MRP8),³⁴ OAT1 and OAT3³⁵ and has also been associated with renal toxicity.² *ABCC10* 526G>A and *ABCC10* 2843T>C have previously been associated with kidney toxicity *in vitro* using HEK-293-ABCC10 cell lines.³⁴ Tenofovir is not a proven substrate of ABCC2; however, *ABCC2* 24C>T and *ABCC2* 1249G>A were found to have protective properties against kidney toxicity in Japanese populations.³⁶ It has been postulated that endogenous substrates of ABCC2 compete with or exacerbate tenofovir transport by ABCC4; furthermore, ABCC2 may be in linkage disequilibrium with other polymorphisms that increase toxicity.³⁷ No significant relationships were evident between tenofovir CL/F and *ABCC10* 526G>A, *ABCC10* 2843T>C, *ABCC2* 24C>T and *ABCC2* 1249G>A in the present study. The impact of *ABCG2* 421C>A on tenofovir has produced conflicting results with one study in HIV-infected women demonstrating a significant increase in AUC_{0-24} in carriers of the rare allele³⁸ whereas another observed lower tenofovir concentrations in plasma and urine of HIV-infected patients of *ABCG2* 421CA genotype compared with homozygotes for the common allele (CC).³⁹ Our investigations found that *ABCG2* 421C>A was significantly associated with 18% lower tenofovir CL/F (increased AUC_{0-24} in CA/AA carriers); however, it did not meet the criteria to remain in the final model. Previous population pharmacokinetic analyses have demonstrated a significant relationship between tenofovir CL/F and CL_{CR} ,^{11,40–42} but this was not replicated here. Although exposure to tenofovir was lower than previously reported, higher tenofovir AUC_{0-24} and C_{max} were associated with decreased glomerular function, but the proportion of patients with reduced function was small. Previous associations between renal function parameters and relevant tenofovir transporter polymorphisms were not replicated in this study.

Emtricitabine is a substrate of the MATE1 transporter in the kidney⁴³ and potentially *SCL47A1* (922–158G>A) rs2289669 G>A could reduce function or expression of MATE1.⁴⁴ The polymorphism has been linked to the response to metformin in patients with type 2 diabetes.⁴⁵ *SCL47A1* rs2289669 G>A did not significantly impact emtricitabine CL/F, although a relationship between emtricitabine CL/F and CL_{CR} was demonstrated, similar to other population pharmacokinetic studies.^{10,40,46}

Study limitations included the use of one sample per patient at Weeks 4 and 24 as this is insufficient to allow adequate partition of random effects (i.e. distinguishing between IIV in parameters and residual variability).⁴⁷ Therefore priors from the literature were

used⁴⁸ and this can be problematic as they may not be informative for the study population and could impact individual parameter estimates. Indeed, model misspecification was noted at the lower concentrations for ritonavir, tenofovir and emtricitabine or during time periods where data were particularly sparse; however, the central tendency of all drugs was well described and darunavir, ritonavir and emtricitabine were within previously reported concentration ranges. Secondly, measurements of intracellular tenofovir diphosphate and emtricitabine triphosphate, the pharmacologically active metabolites of tenofovir and emtricitabine, or tenofovir in urine were not performed in this study. Potentially, these would be more closely related to efficacy or renal impairment assessment, respectively.

In conclusion, within a large cohort of European HIV-infected patients we did not observe a clinically relevant drug–drug interaction between darunavir/ritonavir and raltegravir as part of an NRTI-sparing regimen. Furthermore, darunavir pharmacokinetic parameters were not associated with virological failure. Overall, genetic polymorphisms related to drug metabolism and transport had little impact on darunavir, ritonavir, tenofovir or emtricitabine concentrations. Within the context of the NEAT001/ANRS143 non-inferiority analysis,⁴ these data appear to confirm the potential utility of once-daily darunavir/ritonavir + twice-daily raltegravir as an additional option for treatment-naïve patients without PI-associated viral mutations.

Acknowledgements

Some of these data were presented at HIV Glasgow 2016 (Glasgow, UK, 23–26 October 2016) as poster presentations (Abstracts 305 and 308).

We thank the NEAT001/ANRS143 study participants and their partners, families and caregivers, the staff from all the centres taking part in the trial and all the research staff involved.

Members of the NEAT001/ANRS143 study group

*Indicates staff who left during the trial.

Trial Development Team (TDT): Belgium: Nikos Dedes (Brussels); France: Genevieve Chene, Laura Richert (Bordeaux), Clotilde Allavena, Francois Raffi (Nantes) and Brigitte Autran (Paris); Italy: Andrea Antinori, Raffaella Bucciardini and Stefano Vella (Rome); Poland: Andrzej Horban (Warsaw); Spain: Jose Arribas (Madrid); UK: Abdel G Babiker, Marta Boffito, Deenan Pillay and Anton Pozniak (London). **Trial Steering Committee (TSC):** Belgium: Xavier Franquet* and Siegfried Schwarze (Brussels); Denmark: Jesper Grarup (Copenhagen); France: Genevieve Chene, Aurelie Fischer*, Laura Richert, Cedrick Wallet (Bordeaux), Francois Raffi (Nantes), Alpha Diallo, Jean-Michel Molina and Juliette Saillard (Paris); Germany: Christiane Moecklinghoff (Janssen Pharmaceuticals; Neuss) and Hans-Jurgen Stellbrink (Hamburg); Italy: Stefano Vella (Rome); The Netherlands: Remko Van Leeuwen (Amsterdam); Spain: Jose Gatell (Barcelona); Sweden: Eric Sandstrom (Stockholm); Switzerland: Markus Flepp (Zurich); UK: Abdel G. Babiker, Fiona Ewings*, Elizabeth C. George, Fleur Hudson and Anton Pozniak (London); USA: Gillian Pearce*, Romina Quercia*, Felipe Rogatto (Gilead Sciences; Foster City, CA), Randi Leavitt and Bach-Yen Nguyen* (Merck Laboratories; Whitehouse Station, NJ). **Independent Data Monitoring Committee (IDMC):** Tim Peto (Chair), Oxford, UK; Frank Goebel, Munich, Germany; Simone Marcotullio, Rome, Italy; Veronica Miller, Washington DC, USA; Peter Sasieni, London, UK. **Trial Management Team (TMT):** France: Clotilde Allavena and François Raffi (Nantes); Italy: Stefano Vella (Rome); UK: Anton Pozniak (London). **CMG-EC, INSERM U897**

Coordinating Unit, Bordeaux, France: Genevieve Chêne, Head of coordinating CTU, Member; Fabien Arnault*, Coordinating CTU representative, Member; Céline Boucherie*, Bordeaux CTU representative, Observer; Aurélie Fischer*, Coordinating CTU representative, Member; Delphine Jean*, Bordeaux CTU representative, Observer; Virginie Paniego*, Coordinating CTU representative, Member; Felasoa Paraina, Bordeaux CTU representative, Observer; Laura Richert, Coordinating CTU representative, Member; Elodie Rouch*, Bordeaux CTU representative, Observer; Christine Schwimmer, Coordinating CTU representative, Member; Malika Soussi*, Bordeaux CTU representative, Observer; Audrey Taieb*, Bordeaux CTU representative, Observer; Monique Termote, Coordinating CTU representative, Member; Guillaume Touzeau*, Coordinating CTU representative, Member; Cédric Wallet, Bordeaux CTU representative, Member.

MRC Clinical Trials Coordinating Unit, London, UK: Abdel G. Babiker, Trial Statistician, Member; Adam Cursley, MRC CTU representative, Observer; Wendy Dodds*, MRC CTU representative, Member; Fiona Ewings*, Trial Statistician, Member; Elizabeth C. George, Trial Statistician, Member; Anne Hoppe*, MRC CTU representative, Observer; Fleur Hudson, MRC CTU representative, Member; Ischa Kummeling*, MRC CTU representative, Observer; Filippo Pacciarini*, MRC CTU representative, Observer; Nick Paton*, MRC CTU representative, Observer; Charlotte Russell, MRC CTU representative, Observer; Kay Taylor*, MRC CTU representative, Observer; Denise Ward, MRC CTU representative, Observer. **CHIP Coordinating Unit,**

Copenhagen, Denmark: Representatives: Bitten Aagaard*, Observer; Marius Eid, Observer; Daniela Gey*, Member; Birgitte Gram Jensen*, Observer; Jesper Grarup, Member; Marie-Louise Jakobsen*, Observer; Per O. Jansson, Member; Karoline Jensen*, Member; Zillah Maria Joensen, Observer; Ellen Moseholm Larsen*, Observer; Christiane Pahl*, Observer; Mary Pearson*, Member; Birgit Riis Nielsen, Observer; Søren Stentoft Reilev*, Observer. **Amsterdam Medical Center Coordinating Unit, Amsterdam, The Netherlands:** AMC CTU representatives: Ilse Christ, Observer; Desiree Lathouwers*, Member; Corry Manting, Member; Remko Van Leeuwen, Member. **ANRS, Paris, France:** Alpha Diallo, Pharmacovigilance representative, Member; Bienvenu Yves Mendy*, Pharmacovigilance representative, Member; Annie Metro*, Pharmacovigilance representative, Member; Juliette Saillard, Sponsor representative, Member; Sandrine Couffin-Cadiergues, Sponsor representative, Observer. **ISS, Rome, Italy:** NEAT management representatives: Anne-Laure Knellwolf*, Observer; Lucia Palmisiano, Member. **Local Clinical Trial Units (CTU):** GESIDA, Madrid, Spain: Esther Aznar, Cristina Barea*, Manuel Cotarelo*, Herminia Esteban, Iciar Girbau*, Beatriz Moyano, Miriam Ramirez*, Carmen Saiz, Isabel Sanchez, Maria Yllescas;

ISS, Rome, Italy: Andrea Binelli, Valentina Colasanti, Maurizio Massella, Lucia Palmisiano; **University of Athens Medical School, Greece:** Olga Anagnostou, Vicky Gioukari, Giota Touloumi. **Study Investigators:** Austria: Brigitte Schmid (National Coordinating Investigator), Armin Rieger, Norbert Vetter; Belgium: Stephane De Wit (National Coordinating Investigator), Eric Florence, Linos Vandekerckhove; Denmark: Jan Gerstoft (National Coordinating Investigator), Lars Mathiesen; France: Christine Katlama (National Coordinating Investigator), Andre Cabie, Antoine Cheret, Michel Dupon, Jade Ghosn*, Pierre-Marie Girard, Cécile Goujard, Yves Lévy, Jean-Michel Molina, Philippe Morlat, Didier Neau, Martine Obadia, Philippe Perre, Lionel Piroth, Jacques Reynes, Pierre Tattevin, Francois Raffi, Jean Marie Ragnaud*, Laurence Weiss, Yazdanpanah Yazdan*, Patrick Yeni, David Zucman; Germany: Georg Behrens (National Coordinating Investigator), Stefan Esser, Gerd Fätkenheuer, Christian Hoffmann, Heiko Jessen, Jürgen Rockstroh, Reinhold Schmidt, Christoph Stephan, Stefan Unger; Greece: Angelos Hatzakis (National Coordinating Investigator), George L Daikos, Antonios Papadopoulos, Athamasios Skoutelis; Hungary: Denes Banhegyi (National Coordinating Investigator); Ireland: Paddy Mallon (National Coordinating Investigator), Fiona Mulcahy; Italy: Andrea Antinori (National Coordinating Investigator), Massimo Andreoni, Stefano Bonora,

Francesco Castelli, Antonella D'Arminio Monforte, Giovanni Di Perri, Massimo Galli, Adriano Lazzarin, Francesco Mazzotta, Carlo Torti*, Vincenzo Vullo; **The Netherlands:** Jan Prins (National Coordinating Investigator), Clemens Richter, Dominique Verhagen, Arne Van Eeden*; **Poland:** Andrzej Horban (National Coordinating Investigator); **Portugal:** Manuela Doroana (National Coordinating Investigator), Francisco Antunes*, Fernando Maltez, Rui Sarmento-Castro; **Spain:** Juan González García (National Coordinating Investigator), José López Aldeguer, Bonaventura Clotet, Pere Domingo, Jose M. Gatell, Hernando Knobel, Manuel Marquez, Martin Pilar Miralles, Joaquin Portilla, Vicente Soriano, MariaJesus Tellez; **Sweden:** Anders Thalme (National Coordinating Investigator), Anders Blaxhult, Magnus Gisslen; **UK:** Alan Winston (National Coordinating Investigator), Julie Fox, Mark Gompels. Elbushra Herieka, Margaret Johnson, Clifford Leen, Anton Pozniak, Alastair Teague, Ian Williams. **Endpoint Review Committee (ERC):** **Australia:** Mark Alastair Boyd (Sydney); **Denmark:** Jesper Grarup, Per O. Jansson, Nina Friis Møller and Ellen Frøsig Moseholm Larsen (Copenhagen); **France:** Philippe Morlat (Bordeaux), Lionel Piroth (Dijon) and Vincent Le Moing (Montpellier); **The Netherlands:** Ferdinand W. N. M. Wit, chair (Amsterdam); **Poland:** Justyna Kowalska (Warsaw); **Spain:** Juan Berenguer and Santiago Moreno (Madrid); **Switzerland:** Nicolas J. Müller (Zurich); **UK:** Estée Török (Cambridge), Frank Post (London) and Brian Angus (Oxford). **Sub-study working groups:** **Virology working group:** Vincent Calvez (coordinator), Charles Boucher, Simon Collins, David Dunn (statistician), Sidonie Lambert, Anne-Geneviève Marcelin, Carlo Federico Perno, Deenan Pillay, Ellen White (statistician); **Pharmacology and adherence working group:** Marta Boffito (coordinator), Adriana Ammassari, Andrea Antinori, Wolfgang Stöhr (statistician); **Immunology working group:** Brigitte Autran (coordinator), Reinhold Ernst Schmidt, Michal Odermarsky, Colette Smith, Rodolphe Thiébaud (statistician); **Toxicity, including coinfection working group:** Jose Arribas (coordinator), Jose Ignacio Bernardino De La Serna, Antonella Castagna, Stephane De Wit, Xavier Franquet, Hans-Jacob Furrer, Christine Katlama, Amanda Mocroft (statistician), Peter Reiss; **Quality-of-life working group:** Raffaella Bucciardini (coordinator), Nikos Dedes, Vincenzo Fragola, Elizabeth C. George (statistician), Marco Lauriola, Rita Murri, Pythia Nieuwkerk, Bruno Spire, Alain Volny-Anne, Brian West; **Neurocognitive function working group:** Hélène Amieva (coordinator), Andrea Antinori, Josep Maria Llibre Codina, Laura Richert, Wolfgang Stöhr (statistician), Alan Winston; **Pharmacoeconomics working group:** Francesco Castelli (coordinator), Marco Braggion (statistician), Emanuele Focà.

Funding

NEAT is a project funded to the Instituto Superiore di Sanita, Rome, by the European Union under the Sixth Framework Programme, project number LSHP-CT-2006-037570. The trial was also supported by Gilead Sciences, Janssen Pharmaceuticals, and Merck Laboratories and The French National Institute for Health and Medical Research, France. Recherche Nord&Sud Sida-HIV Hepatites (Inserm-ANRS) is the sponsor and a funder of the trial.

Transparency declarations

S.B. and G.D.P. have received research grants, travel grants, and consultancy fees from Abbvie, Boehringer-Ingelheim, Bristol-Myers Squibb, Merck Sharp & Dohme, Gilead Sciences, Janssen-Cilag and ViiV Healthcare. A.O. has received research funding income from ViiV Healthcare, Merck, and Janssen, as well as consultancies from ViiV Healthcare and Merck. He is also a co-inventor of patents relating to the

use of nanotechnology in drug delivery, and is a director of Tandem Nano Ltd. J.-M.M. and F.R. have received advisory or invited speaker honoraria and have received research grants from Abbvie, Bristol-Myers Squibb, Gilead Sciences, Janssen Pharmaceuticals, Merck Laboratories, Merck Sharp & Dohme, Tobira and ViiV Healthcare. A.P. has received research funding income from ViiV Healthcare, Merck, Gilead and Janssen, was NEAT co-chair and has participated in advisory boards and symposia for ViiV Healthcare, Gilead, Janssen and Merck. L.R. is involved in IMI-2 funded Ebovac2 and Ebovac3 consortia on Ebola vaccine development, in which Janssen is the industrial partner, and in a publicly funded and sponsored Ebola vaccine trial (Prevac trial) for which Janssen and Merck provide the investigational products (vaccines). M.B. has received travel and research grants from and has been advisor for Janssen, Roche, ViiV, Bristol-Myers Squibb, Merck Sharp & Dohme, Gilead Sciences, Mylan, Cipla and Teva. All other authors: none to declare.

Author contributions

L.D., population pharmacokinetic modelling strategy and analysis, manuscript preparation; R.G., DNA extraction, genotyping, manuscript preparation; W.S., statistical analysis, manuscript preparation; S.B., pharmacokinetic bioanalysis, manuscript review; A.O., funding, strategy and supervision of pharmacogenetic analysis, genetic data review, manuscript review; A.D., pharmacokinetic bioanalysis, pharmacokinetic data review, manuscript review; A.C., study management, statistical review, manuscript review; J.-M.M., patient enrolment, manuscript review; G.F., patient enrolment, manuscript review; L.V., patient enrolment, manuscript review; G.D.P., study design, protocol review, patient enrolment, manuscript review; A.P., study design, protocol review, patient enrolment, manuscript review; L.R., study design, protocol review, manuscript review; F.R., study design, protocol review, patient enrolment, manuscript review; M.B., pharmacokinetic sub-study lead, study design, protocol review, patient enrolment, manuscript review.

Supplementary data

Tables S1–S4 and Figures S1–S4 are available as [Supplementary data](#) at JAC Online.

References

- 1 EACS: European AIDS Clinical Society. EACS Guidelines 2018. http://www.eacsociety.org/files/2018_guidelines-9.1-english.pdf.
- 2 Hall AM, Hendry BM, Nitsch D *et al.* Tenofovir-associated kidney toxicity in HIV-infected patients: a review of the evidence. *Am J Kidney Dis* 2011; **57**: 773–80.
- 3 McComsey GA, Tebas P, Shane E *et al.* Bone disease in HIV infection: a practical review and recommendations for HIV care providers. *Clin Infect Dis* 2010; **51**: 937–46.
- 4 Raffi F, Babiker AG, Richert L *et al.* Ritonavir-boosted darunavir combined with raltegravir or tenofovir-emtricitabine in antiretroviral-naïve adults infected with HIV-1: 96 week results from the NEAT001/ANRS143 randomised non-inferiority trial. *Lancet* 2014; **384**: 1942–51.
- 5 D'Avolio A, Sciandra M, Siccardi M *et al.* A new assay based on solid-phase extraction procedure with LC-MS to measure plasmatic concentrations of tenofovir and emtricitabine in HIV infected patients. *J Chromatogr Sci* 2008; **46**: 524–8.
- 6 D'Avolio A, Siccardi M, Sciandra M *et al.* HPLC-MS method for the simultaneous quantification of the new HIV protease inhibitor darunavir, and 11 other antiretroviral agents in plasma of HIV-infected patients. *J Chromatogr B Analyt Technol Biomed Life Sci* 2007; **859**: 234–40.

- 7 Olagunju A, Bolaji O, Amara A et al. Pharmacogenetics of pregnancy-induced changes in efavirenz pharmacokinetics. *Clin Pharmacol Ther* 2015; **97**: 298–306.
- 8 Beal S, Sheiner LB, Boeckmann AJ et al. *NONMEM Users Guide 2013*. ICON Development Solutions, 1989–2013.
- 9 Moltó J, Xinarianos G, Miranda C et al. Simultaneous pharmacogenetics-based population pharmacokinetic analysis of darunavir and ritonavir in HIV-infected patients. *Clin Pharmacokinet* 2013; **52**: 543–53.
- 10 Valade E, Treluyer JM, Bouazza N et al. Population pharmacokinetics of emtricitabine in HIV-1-infected adult patients. *Antimicrob Agents Chemother* 2014; **58**: 2256–61.
- 11 Baheti G, Kiser JJ, Havens PL et al. Plasma and intracellular population pharmacokinetic analysis of tenofovir in HIV-1-infected patients. *Antimicrob Agents Chemother* 2011; **55**: 5294–9.
- 12 Bergstrand M, Hooker AC, Wallin JE et al. Prediction-corrected visual predictive checks for diagnosing nonlinear mixed-effects models. *AAPS J* 2011; **13**: 143–51.
- 13 Lindbom L, Pihlgren P, Jonsson EN. PsN-Toolkit—a collection of computer intensive statistical methods for non-linear mixed effect modeling using NONMEM. *Comput Methods Programs Biomed* 2005; **79**: 241–57.
- 14 Jonsson EN, Karlsson MO. Xpose—an S-PLUS based population pharmacokinetic/pharmacodynamic model building aid for NONMEM. *Comput Methods Programs Biomed* 1999; **58**: 51–64.
- 15 White IR, Royston P. Imputing missing covariate values for the Cox model. *Statist Med* 2009; **28**: 1982–98.
- 16 Dickinson L, Boffito M, Back D et al. Sequential population pharmacokinetic modeling of lopinavir and ritonavir in healthy volunteers and assessment of different dosing strategies. *Antimicrob Agents Chemother* 2011; **55**: 2775–82.
- 17 Kakuda TN, Brochot A, Tomaka FL et al. Pharmacokinetics and pharmacodynamics of boosted once-daily darunavir. *J Antimicrob Chemother* 2014; **69**: 2591–605.
- 18 Gilead Science Ltd. Emtriva (emtricitabine) 200 mg hard capsules Summary of Product Characteristics. 2019. <https://www.medicines.org.uk/emc/product/18/smpc>.
- 19 Gilead Science Ltd. Viread (tenofovir disoproxil fumarate) 245 mg film-coated tablets Summary of Product Characteristics. 2019. <https://www.medicines.org.uk/emc/product/1615/smpc>.
- 20 Cattaneo D, Gervasoni C, Cozzi V et al. Co-administration of raltegravir reduces daily darunavir exposure in HIV-1 infected patients. *Pharmacol Res* 2012; **65**: 198–203.
- 21 Fabbiani M, Di Giambenedetto S, Ragazzoni E et al. Darunavir/ritonavir and raltegravir coadministered in routine clinical practice: potential role for an unexpected drug interaction. *Pharmacol Res* 2011; **63**: 249–53.
- 22 Garvey L, Latch N, Erlwein OW et al. The effects of a nucleoside-sparing antiretroviral regimen on the pharmacokinetics of ritonavir-boosted darunavir in HIV type-1-infected patients. *Antivir Ther* 2010; **15**: 213–8.
- 23 Hartkoorn RC, Kwan WS, Shallcross V et al. HIV protease inhibitors are substrates for OATP1A2, OATP1B1 and OATP1B3 and lopinavir plasma concentrations are influenced by SLCO1B1 polymorphisms. *Pharmacogenet Genomics* 2010; **20**: 112–20.
- 24 Elens L, van Gelder T, Hesselink DA et al. CYP3A4*22: promising newly identified CYP3A4 variant allele for personalizing pharmacotherapy. *Pharmacogenomics* 2013; **14**: 47–62.
- 25 Hustert E, Haberl M, Burk O et al. The genetic determinants of the CYP3A5 polymorphism. *Pharmacogenetics* 2001; **11**: 773–9.
- 26 Kuehl P, Zhang J, Lin Y et al. Sequence diversity in CYP3A promoters and characterization of the genetic basis of polymorphic CYP3A5 expression. *Nat Genet* 2001; **27**: 383–91.
- 27 Olagunju A, Schipani A, Siccardi M et al. CYP3A4*22 (c.522-191 C>T; rs35599367) is associated with lopinavir pharmacokinetics in HIV-positive adults. *Pharmacogenet Genomics* 2014; **24**: 459–63.
- 28 Lu Y, Fuchs EJ, Hendrix CW et al. CYP3A5 genotype impacts maraviroc concentrations in healthy volunteers. *Drug Metab Dispos* 2014; **42**: 1796–802.
- 29 Schipani A, Siccardi M, D'Avolio A et al. Population pharmacokinetic modeling of the association between 63396C→T pregnane X receptor polymorphism and unboosted atazanavir clearance. *Antimicrob Agents Chemother* 2010; **54**: 5242–50.
- 30 Arab-Alameddine M, Lubomirov R, Fayet-Mello A et al. Population pharmacokinetic modelling and evaluation of different dosage regimens for darunavir and ritonavir in HIV-infected individuals. *J Antimicrob Chemother* 2014; **69**: 2489–98.
- 31 Browne RW, Rosenkranz SL, Wang Y et al. Sources of variability and accuracy of performance assessment in the clinical pharmacology quality assurance proficiency testing program for antiretrovirals. *Ther Drug Monit* 2019; **41**: 452–8.
- 32 Kohler JJ, Hosseini SH, Green E et al. Tenofovir renal proximal tubular toxicity is regulated by OAT1 and MRP4 transporters. *Lab Invest* 2011; **91**: 852–8.
- 33 Tun-Yhong W, Chinpaisal C, Pamonsinlapatham P et al. Tenofovir disoproxil fumarate is a new substrate of ATP-binding cassette subfamily C member 11. *Antimicrob Agents Chemother* 2017; **61**: e01725–16.
- 34 Pushpakom SP, Liptrott NJ, Rodriguez-Novoa S et al. Genetic variants of ABCB10, a novel tenofovir transporter, are associated with kidney tubular dysfunction. *J Infect Dis* 2011; **204**: 145–53.
- 35 Uwai Y, Ida H, Tsuji Y et al. Renal transport of adefovir, cidofovir, and tenofovir by SLC22A family members (hOAT1, hOAT3, and hOCT2). *Pharm Res* 2007; **24**: 811–5.
- 36 Nishijima T, Komatsu H, Higasa K et al. Single nucleotide polymorphisms in ABCB2 associate with tenofovir-induced kidney tubular dysfunction in Japanese patients with HIV-1 infection: a pharmacogenetic study. *Clin Infect Dis* 2012; **55**: 1558–67.
- 37 Moss DM, Neary M, Owen A. The role of drug transporters in the kidney: lessons from tenofovir. *Front Pharmacol* 2014; **5**: 248.
- 38 Baxi SM, Greenblatt RM, Bacchetti P et al. Evaluating the association of single-nucleotide polymorphisms with tenofovir exposure in a diverse prospective cohort of women living with HIV. *Pharmacogenomics J* 2018; **18**: 245–50.
- 39 Bracchi M, Neary M, Pagani N et al. ABCG2 rs231142 influences TFV concentrations in plasma and urine. *Conference on Retroviruses and Opportunistic Infections (CROI), Seattle, WA, USA, 2017*. Abstract 418.
- 40 Dickinson L, Yapa HM, Jackson A et al. Plasma tenofovir, emtricitabine, and rilpivirine and intracellular tenofovir diphosphate and emtricitabine triphosphate pharmacokinetics following drug intake cessation. *Antimicrob Agents Chemother* 2015; **59**: 6080–6.
- 41 Lu Y, Goti V, Chaturvedula A et al. Population pharmacokinetics of tenofovir in HIV-1-uninfected members of serodiscordant couples and effect of dose reporting methods. *Antimicrob Agents Chemother* 2016; **60**: 5379–86.
- 42 Punyawudho B, Thammajaruk N, Thongpeang P et al. Population pharmacokinetics of tenofovir in HIV/HBV co-infected patients. *Int J Clin Pharmacol Ther* 2015; **53**: 947–54.
- 43 Reznicek J, Ceckova M, Cerveny L et al. Emtricitabine is a substrate of MATE1 but not of OCT1, OCT2, P-gp, BCRP or MRP2 transporters. *Xenobiotica* 2017; **47**: 77–85.

- 44** Becker ML, Visser LE, van Schaik RH *et al*. Interaction between polymorphisms in the OCT1 and MATE1 transporter and metformin response. *Pharmacogenet Genomics* 2010; **20**: 38–44.
- 45** Tkac I, Klimcakova L, Javorsky M *et al*. Pharmacogenomic association between a variant in SLC47A1 gene and therapeutic response to metformin in type 2 diabetes. *Diabetes Obes Metab* 2013; **15**: 189–91.
- 46** Valade E, Treluyer JM, Illamola SM *et al*. Emtricitabine seminal plasma and blood plasma population pharmacokinetics in HIV-infected men in the EVARIST ANRS-EP 49 study. *Antimicrob Agents Chemother* 2015; **59**: 6800–6.
- 47** Ette EI, Kelman AW, Howie CA *et al*. Analysis of animal pharmacokinetic data: performance of the one point per animal design. *J Pharmacokinet Biopharm* 1995; **23**: 551–66.
- 48** Gislenskog PO, Karlsson MO, Beal SL. Use of prior information to stabilize a population data analysis. *J Pharmacokinet Pharmacodyn* 2002; **29**: 473–505.